# Journal of Applied Sciences

ISSN 1812-5654

science alert

ANSInet
an open access publisher
http://ansinet.com

Journal of Applied Sciences 10 (1): 20-28, 2010
ISSN 1812-5654


# Simulation of Three Different Double-Fiber Probes for Reflection Sensing

[1]R. Jafari and [2]H. Golnabi
[1]Plasma Physics Research Center, Science and Research Branch,
Islamic Azad University, P.O. Box 14665-678, Tehran, Iran
[2]Institute of Water and Energy, Sharif University of Technology, P.O. Box 11155-8639, Tehran, Iran

**Abstract:** In this study simulation results for three double-fiber optical designs for the reflection measurements are reported. Modeling is perused for three cases namely Equal Fibers (EF), transmitter fiber shorter (TS) and receiver fiber shorter (RS) designs. By proper modeling and written programs the operations of such symmetric double-fiber probes are simulated and the role of different crucial parameters such as fiber-to-fiber distance (t), fiber core radius (r) and fiber Numerical Aperture (NA) are investigated. In the second study simulation results for the transmitter fiber shorter and receiver fiber shorter designs are investigated for different fiber length differences (w). Finally simulation results for the three different designs of equal fibers, transmitter shorter and receiver fiber shorter probes are compared and optimum conditions are described. All three arrangements simulated here offer valuable results for sensing operations such as reflection or displacement measurements. However, the RS probe geometry offers a better design with the less dead region in comparison with the EF and TS designs.

**Key words:** Reflection, target, fiber, beam overlap, simulation

## INTRODUCTION

Recently a variety of optical systems have been reported in literature for different sensing applications (Yuan *et al*., 2009; Babchenko and Maryles, 2007; Baptista *et al*., 2006; Peng *et al*., 2005; Donlagić and Cibula, 2005; Qiu *et al*., 2004). Some of the successful optical designs are reported, which are based on the intensity modulation technique and used fibers as waveguide in sensing operations (Golnabi, 2002; Golnabi and Jafari, 2006; Golnabi *et al*., 2007; Golnabi, 2000a; Golnabi and Azimi, 2007). The ease of operation, cost factor and precise performance requirements has led to the design of the plastic fibers in a double-fiber probe (Golnabi and Azimi, 2008). The double fiber design in spite of small probe size can be used for local and remote non-contact distance measurements that are required in many applications. The reported simulation results are based on a design that uses the intensity modulation of reflected light from a surface and it can be used in different applications. Considering the importance of such a double fiber system in this article we report simulation results obtained by variation of different important parameters controlling the system performance and merits. The goal of this study is to provide some simulation result, which leads to the optimum situation in using such an optical fiber sensor. The reported simulation results can offer some advantages concerning the optimization of crucial parameter which can be helpful in design and construction of similar displacement sensors.

## MATERIALS AND METHODS

Development of the reported method and related computations are performed for the period of 2008-9. The double-fiber designs used in this modeling consist of a pair of similar plastic optical fibers (Weinert, 1999). As can be seen in Fig. 1, a double fiber assembly is used in this modeling in which in one end; two fibers are separated and they are close to each other at the other end. At this end two fibers are attached side-by-side together to form a single double fiber. The double end is mounted in a fixed holder assembly in line with the reflecting target. The separated fiber ends can be connected to the light source and photodetector accordingly. More experimental details about double fiber usage can be found in other references (Golnabi and Azimi, 2008). All the double fiber assemblies shown in Fig. 1a-c include similar plastic optical step-index fibers. The overall diameter of each fiber is estimated to be about 2.2 mm and the typical core diameter considered to be about 860 μm in order to be compatible with the practical values (Golnabi and Azimi, 2008).

As shown in Fig. 1a the first double-fiber probe denoted as EF has an equal size for the transmitter and

**Corresponding Author:** Roya Jafari, Plasma Physics Research Center, Science and Research Branch, Islamic Azad University, P.O. Box 14665-678, Tehran, Iran Tel: +98 21 44869627 Fax: +98 21 44817165

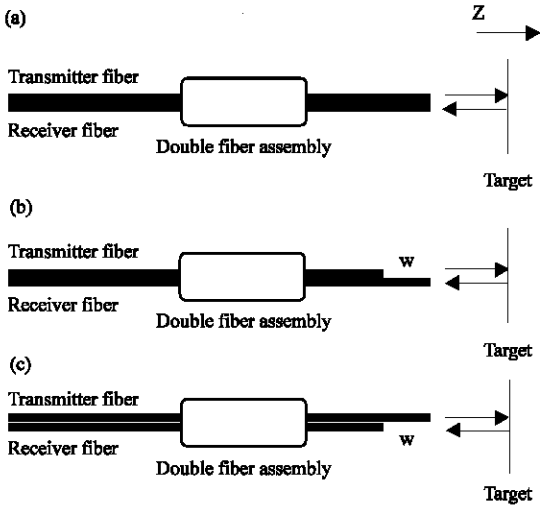


Fig. 1: Double fiber arrangements. (a) Equal fibers design (EF), (b) Transmitter fiber Shorter (TS) and (c) Receiver fiber Shorter (RS)

receiver fibers. The second arrangement shown in Fig. 1b is denoted as TS in which the transmitter fiber is shorter than the receiver fiber by amount of w. The third arrangement shown in Fig. 1c is denoted as RS in which the receiver fiber is shorter than the transmitter fiber by the same amount of w. From now on we refer to these cases as EF, TS and RS designs, respectively.

The reflection concept of light from a surface for this case based on the geometrical optic can be determined from Fig. 2a. The fiber-to-fiber distance indicated in Fig. 2a by t, which is one of the variables of the parametric studies. The distance t for the probe can be varied from 0-3 mm. The core radius of each fiber is another parameter of this study which can be varied from 100-500 μm. The NA of the fiber in double fiber assembly is also varied and simulation results are reported for such variations. Similar parameter studies are performed for TS and RS designs. In addition for such designs length difference denoted by W in Fig. 1b and c are varied and the computed results are compared.

Operation of the modeled double-fiber sensor designs is based on the intensity modulation of the light reflected off the target. In Fig. 2a the image of the transmitted light on the entrance plane (image plane) of the receiving fiber is displayed for EF case. Let us consider the beam cross section on the target plane to be circular in the XY-plane, where Z-axis shows the direction of the propagation of beam. If $r_1$ and $r_2$ represent the transmitter (T-fiber) and receiver fibers (R-fiber) core radius, respectively, then the overlap of two circles

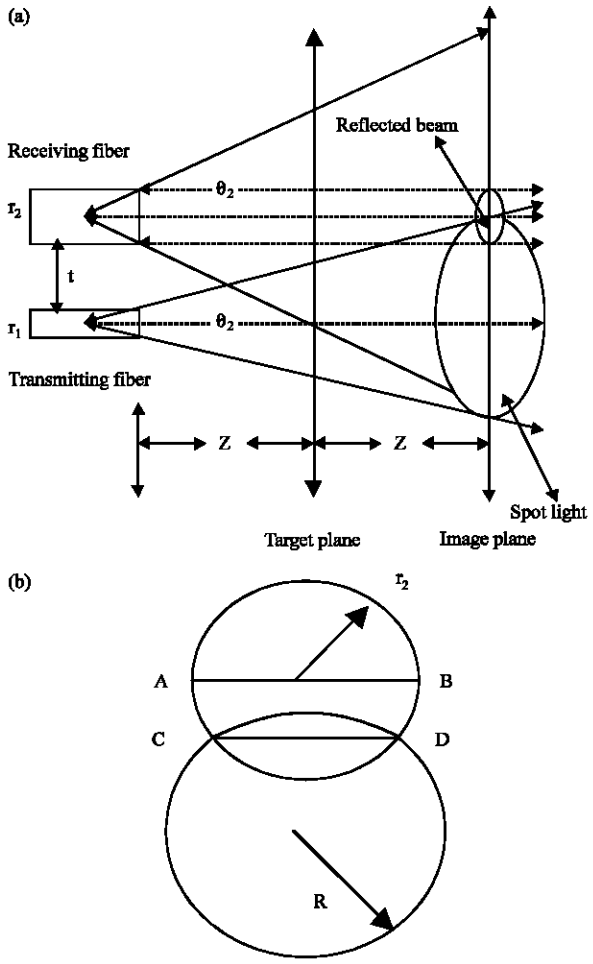


Fig. 2: Light reflection diagram for the case of EF design. (a) Spot light on the image plane or receiving fiber. (b) Cross sectional overlap of the spot light image and receiving fiber

determines the amount of light received by the receiver fiber. For our case in Fig. 2a, we assume $r_1 = r_2$ for similar transmitter and receiver fibers.

Four distinct cases can be considered for such an analysis, as shown in Fig. 2b. Considering first case (a) when there is no crossing of two circles then no specular light is received by the R-fiber (dead region). Second case where there is a possible crossing in two different situations. Diameter AB is either above crossing line CD, case (b) or below the crossing line CD of two circles, case (c). In the last case (d) the small circle can be completely inside the spot light circle. Actually the amount of received light depends on the overlapping area between these two circles. Using geometrical relation one can compute overlapping cross section ΔS for the four described cases. For case a with no overlap one can write:

$$\Delta S = 0 \quad (1)$$

For case b with small overlap where AC line is above CD we have:

$$\Delta S = R^2 \mathrm{Sin}^{-1}(y/R) + r_2^2 \mathrm{Sin}^{-1}(y/r_2) - xy \quad (2)$$

where, R is the radius of the spot light on the target plane (Fig. 2b). Parameters x, R and y are defined as followings:

$$x = r_1 + r_2 + t \quad (3)$$

$$R = r_1 + 2Z\tan\theta_1 \quad (4)$$

$$y = [R^2 - (\frac{x^2 + R^2 - r_2^2}{2x})^2]^{1/2} \quad (5)$$

For case c where AD is below the interception line CD we write:

$$\Delta S = \pi r_2^2 - [r_2^2 \mathrm{Sin}^{-1}(y/r_2) + xy - R^2 \mathrm{Sin}^{-1}(y/R) \quad (6)$$

where, x and R are as above and y is given as:

$$y = [r_2^2 - (\frac{R^2 - r_2^2 - x^2}{2x})^2]^{1/2} \quad (7)$$

For the case of d when small circle is inside the spot light circle we can write:

$$\Delta S = \pi r_2^2 \quad (8)$$

Thus $\Delta S$ can vary from zero from Eq. 1 to a maximum value given by Eq. 8. The received power of the light on the target plane for the case a to c is equal to:

$$P_t = I_0 \Delta S \quad (9)$$

where, $I_0$ is the launching intensity by the T-fiber at the target plane. The reflected intensity from the target plane to be received by the R-fiber is obtained by:

$$I = \rho I_0 \frac{\Delta S}{\pi r_2^2} \quad (10)$$

where, $\rho$ shows the reflection coefficient for the target plane. Theoretical result indicates that by increasing axial distance the collected intensity is increased and at a certain distance reaches a maximum. For the case d intensity variation with distance is given by:

$$I = \frac{\rho I_0}{Z^2} \quad (11)$$

where, Z is the axial distance and Eq. 11 is just the regular intensity decreasing rule. As can be seen the light intensity entered in the receiving fiber varies by the axial distance and as a result in simulation the reflected intensity is plotted as a function of this variable.

## SIMULATION RESULTS

All the reported results are computations based on the developed formulas accomplished by different written programs using the MATLAB software. In the first study simulation results for the case of EF design are reported. Figure 3 shows the computed reflected intensity for a target as of function of the axial distance Z for different fiber-to-fiber distance values, t. The assumed parameters in this computation are NA = 0.2 and r = 430 μm. Intensity variation is considered for the case of t = 1, 2 and 3 mm in the computations and variation are plotted for Z variation of about 24 mm. For all curves shown in Fig. 3, the respond curve starts from a near zero value and reaches a maximum at a particular axial distance and then drops slowly to a minimum value. As can be seen in Fig. 3, by increasing the t value three major changes occur in the intensity plot. First the dead region distance is increased by increasing the t value. For example for t = 1 mm the dead region starts from zero to about 2.5 mm while for the t-value of 3 mm the dead region is from zero to about 7 mm. Second point and perhaps the most important difference, is the shift of the peak intensity to longer distances by increasing the t-value. For instance, for t equal to 1 mm the peak is located to about 4 mm while it is

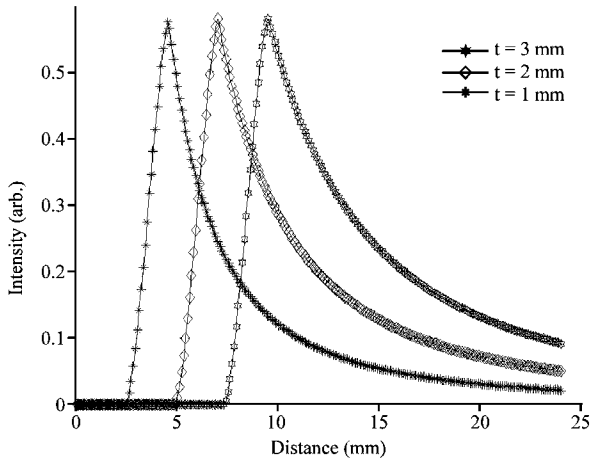


Fig. 3: Reflection intensity as a function of axial distance for different t values for EF design

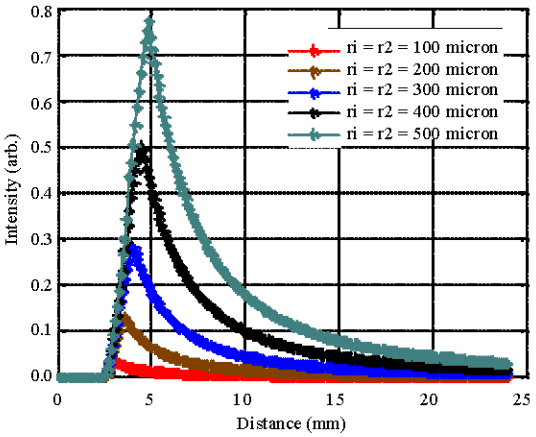


Fig. 4: Reflection intensity as a function of axial distance for different radius r values for EF design

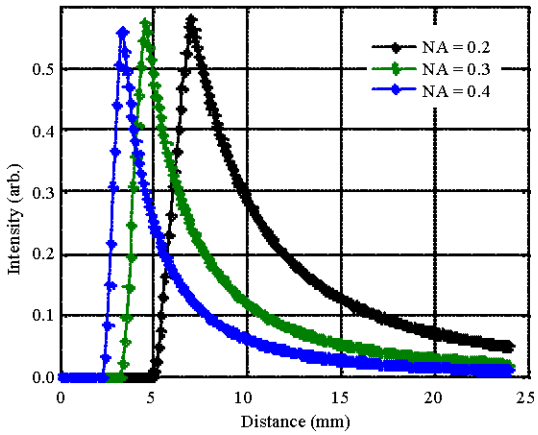


Fig. 5: Reflection intensity versus axial distance for different NA values for EF design

shifted to about 9 mm for the t-value of 3 mm. Third notable points of this study is the variation the bandwidth (FWHM) values for different respond curves. By increasing the t value as can be seen in Fig. 3, the amount of the intensity peak remain constant while the curve bandwidth (FWHM) is considerably increased by increasing the t value. Since all curves obey the same behavior for the falling parts, therefore the observed increase in bandwidth is as a result of the slowing variation of the raising part of the intensity curve with respect to this parameter.

In Fig. 4 the computed reflected intensity as a function of axial distance Z is presented for different r values for EF probe. For this case the assumed parameters in computation are t = 1 mm and NA = 0.2. Intensity variation is considered for the case of r = 100, 200, 300, 400 and 500 μm in the computations and variation are plotted for Z variation of about 24 mm. For all curves shown in Fig. 4, the respond curve starts from a near zero value and reaches a maximum at a particular axial distance and then drops slowly to a minimum vale. As can be seen in Fig. 4, by increasing the fiber core radius value, r, some observations can be made in the intensity plots. First the dead region distance remains constant by increasing the r value.

Second point and perhaps the most important difference, is the shift of the peak intensity to longer distances by increasing the r value. For instance, for r equal to 100 μm the peak is located to about 3 mm while it is shifted to about 5 mm for the r value of 500 μm. Third point and also important one, is the increase of the peak intensity as a result of the r changes. For example, for r equal to 100 μm the maximum peak is about 0.02 on the arbitrary scale while it is increased to about 0.78 on the same scale for the r value of 500 μm. Another notable point of this study is the variation of the bandwidths (FWHM) values for different respond curves. By increasing the r value as can be seen in Fig.4, the amount of the curve bandwidth (FWHM) is increased accordingly. Since all the intensity curves obey the same behavior for the falling part, therefore the observed increase in the bandwidth is due to the slower variation of the raising part of the intensity curve with respect to r.

In Fig. 5 the computed reflected signal intensity for a target as a function of the scan distance Z for different fiber numerical aperture, NA, values for the same EF design are presented. The assumed parameters in this computation are t = 1 mm and r = 430 μm. Intensity variation is considered for the case of NA = 0.2, 0.3 and 0.4 in the computations and variations are plotted for Z variation of about 24 mm. As shown in Fig. 5, the respond curves start from a near zero value and reach a maximum at a particular axial distance and then drop slowly to a minimum vale. As can be seen in Fig. 5, by increasing the numerical aperture value three major changes occur in the intensity plot. First the dead region distance is decreased by increasing the NA value. For example for NA = 0.2 the dead region starts from zero to about 5 mm while for the NA value of 0.4 the dead region is for zero to 2.5 mm. Second point and perhaps the most important difference, is the shift of the peak intensity to longer distances by decreasing the NA value. For instance, for NA equal to 0.4 the peak is located to about 3 mm while it is shifted to about 7 mm for the NA value of 0.2. Other notable points of this study are the variation of the maximum and the bandwidths (FWHM) values for different respond curves. By increasing the NA value as can be seen in Fig. 5, the amount of the intensity peak is slightly reduced while the

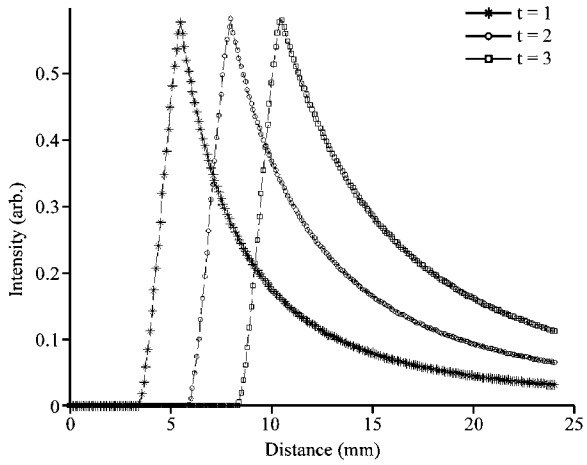


Fig. 6: Reflection intensity as a function of axial distance for different t values for TS design

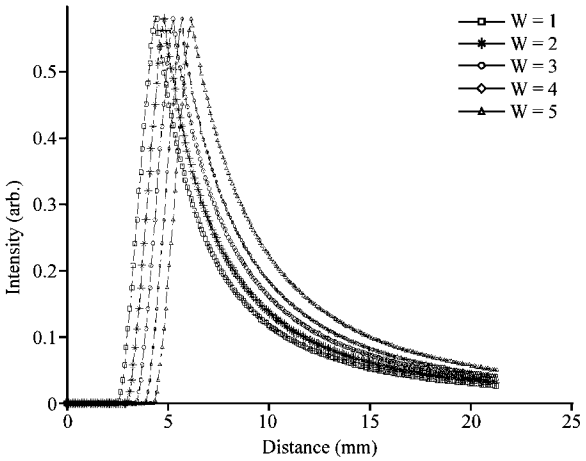


Fig. 7: Reflection intensity as a function of axial distance for different w values for TS design

curve bandwidth (FWHM) is considerably reduced by increasing the NA value. Since both curves obey the same behavior for the falling part, therefore the observed decrease in bandwidth is as a result of the sharpening of the raising part of the intensity curve.

In the next study simulation results for the TS probe are given. Figure 6 shows the computed reflected intensity for a target as a function of the axial distance Z for different fiber-to-fiber t values. For this case the assumed parameters in computation are NA = 0.2, r = 430 μm w = 2 mm. Intensity variation is considered for the case of t = 0, 1, 2 and 3 mm in the computations for TS design and variation are plotted for Z variation of about 24 mm. For all curves shown in Fig. 6, each respond curve starts from a near zero value and reaches a maximum at a particular axial distance and then drops slowly to a minimum vale. As can be seen in Fig. 6, by increasing the t value three major changes occur in the intensity plot. First the dead region distance is increased by increasing the t value (compare to Fig. 3 for EF design). For example for t = 1 mm the dead region starts from zero to about 3.5 mm while for the t value of 3 mm the dead region is from zero to about 8 mm. Second point and perhaps the most important difference, is the shift of the peak intensity to longer distances by increasing the t value. For instance, for t equal to 1 mm the peak is located to about 6 mm while it is shifted to about 11 mm for the t value of 3 mm. Third notable points of this study is the variation the bandwidth (FWHM) values for different respond curves. By increasing the t value as can be seen in Fig. 6, the amount of the intensity peak remain almost constant while the curve bandwidth (FWHM) is considerably increased by increasing the t value. Since all curves obey the same behavior for the falling parts, therefore the observed increase in bandwidth is as a result of the slowing variation of the raising part of the intensity curve with respect to this parameter.

In Fig. 7 the computed reflected intensity for a target as a function of the scan distance Z for different fibers length difference, w, values for the similar TS design is shown. For this study the assumed parameters in computation are t = 1 mm, NA = 0.2, r = 430 μm. In this study role of length difference in computation results are investigated. Intensity variation is considered for the case of w = 1, 2, 3, 4 and 5 mm in the computations and variation are plotted for Z variation of about 24 mm. For all curves shown in Fig. 7, the respond curve starts from a near zero value and reaches a maximum at a particular axial distance and then drops slowly to a minimum vale. As can be seen in Fig. 7, by increasing the length difference, w, value three major changes occur in the intensity curves. First, the dead region distance is increased by increasing the w value. For example for w = 1 mm the dead region starts from zero to about 3 mm while for the w value of 5 mm the dead region is from zero to about 5.0 mm. Second point and perhaps the most important difference, is the shift of the peak intensity to longer distances by increasing the w value. For instance, for w equal to 1 mm the peak is located to about 5 mm while it is shifted to about 7 mm for the w value of 2 mm. Other notable points of this study are the variation of the maximum and the bandwidths (FWHM) values for different respond curves. By increasing the w value as can be seen in Fig. 7, the amount of the intensity peaks remain constant while the curve bandwidth (FWHM) is nearly constant as can be seen in Fig. 7.

The simulation results for the RS probe design are presented. Figure 8 displays the computed reflected intensity for a target as a function of the scan distance, Z,

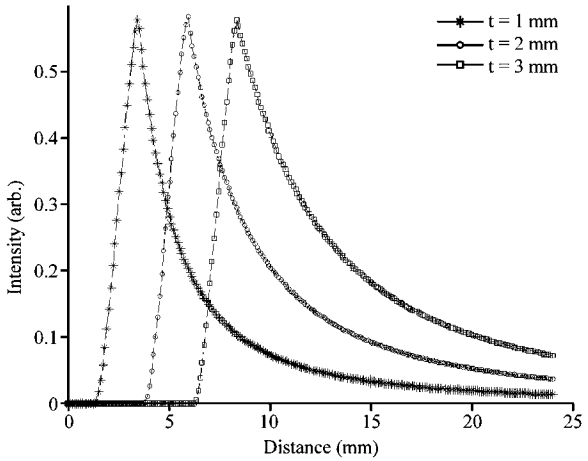


Fig. 8: Reflection intensity versus axial distance for different t values for RS design

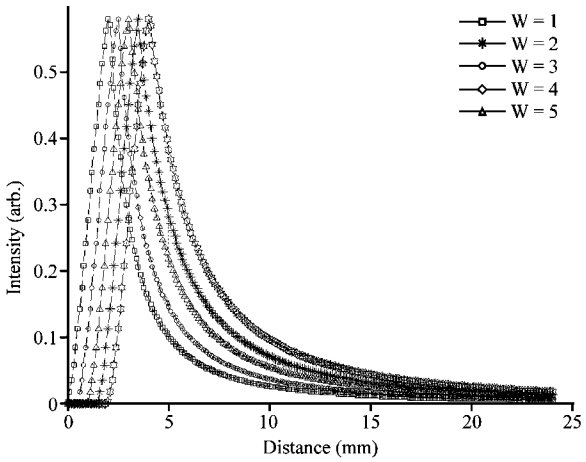


Fig. 9: Reflection intensity versus axial distance for different w values for RS design

for different fiber-to-fiber, t values. For this case the assumed parameters in computation are NA = 0.2, r = 430 μm and w = 2 mm. Intensity variation is considered for the case of t = 0, 1, 2 and 3 mm in the computations for RS design and variation are plotted for Z variation of about 24 mm. For all curves shown in Fig. 8, each respond curve starts from a near zero value and reaches a maximum at a particular axial distance and then drops slowly to a minimum vale. As can be seen in Fig. 8, by increasing the t value as stated before three major changes occur in the intensity plots. First the dead region distance is increased by increasing the t value (compare to Fig. 3 for EF and Fig. 6 for TS design). For example for t = 1 mm the dead region starts from zero to about 1.5 mm while for the t value of 3 mm the dead region is from zero to about 6 mm. Second point and perhaps the most important difference, is the shift of the peak intensity to longer distances by increasing the t value. For instance, for t equal to 1 mm the peak is located to about 3 mm while it is shifted to about 8 mm for the t value of 3 mm. Third notable points of this study is the variation the bandwidth (FWHM) values for different respond curves. By increasing the t value as can be seen in Fig. 8, the amount of the intensity peak remain almost constant while the curve bandwidth (FWHM) is considerably increased by increasing the t value. Since all curves obey the same behavior for the falling parts, therefore the observed increase in bandwidth is as a result of the slowing variation of the raising part of the intensity curve with respect to this parameter.

In Fig. 9 the computed reflected intensity for a target as a function of the axial distance, Z, for different fiber length differences, w, values for the same RS design is displayed. For this investigation the assumed parameters are NA = 0.2, r = 430 μm and t = 1 mm. In this study role of length difference in computation results are investigated for the RS probe design. Intensity variation is considered for the case of w = 1, 2, 3, 4 and 5 mm in the computations and variation are plotted for Z variation of about 24 mm. For all curves shown in Fig. 9, the respond curve starts from a near zero value and reaches a maximum at a particular axial distance and then drops slowly to a minimum of zero value. As can be seen in Fig. 9, by increasing the length difference, w, value three major changes occur in the intensity curves. First the dead region distance is considerably decreased by increasing the w value. For example for w = 1 mm the dead region starts from zero to about 2 mm while for the w value of 5 mm the dead region is very short close to near zero (compare results with that of Fig. 7). Second point and perhaps the most important difference, is the shift of the peak intensity to shorter distances by increasing the w value (The results for Fig. 7). For instance, for w equal to 1 mm the peak is located to about 4 mm while it is reduced to about 2 mm for the w value of 5 mm. Other notable points of this study are the variation of the maximum and the bandwidths (FWHM) values for different respond curves. By increasing the w value as can be seen in Fig. 9, similar to the case of TS design, the amount of the intensity peaks remain constant while the curve bandwidth (FWHM) is nearly constant as can be seen in Fig. 9.

In the last study simulation results for three types probes are compared. Figure 10 shows this comparison of the reflection intensities as a function of axial distance Z for designated EF, TS and RS designs. For all cases the assumed common parameters in computation are t = 1 mm, NA = 0.2 and r = 430 μm and w = 2 mm for TS and RS designs. It is easier to see the role of length difference in

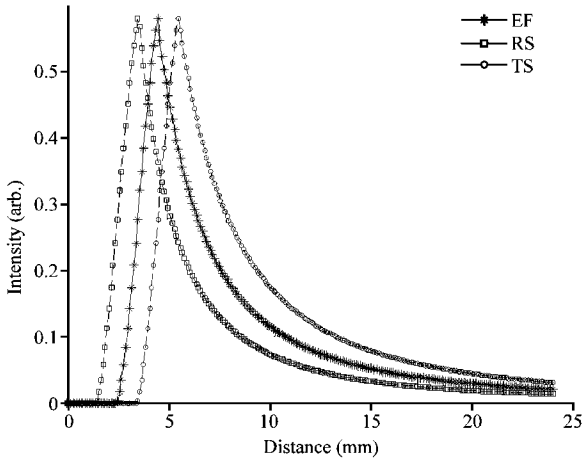


Fig. 10: Comparison of the reflection intensities for different EF, TS and RS designs

this comparison. As usual intensity variation is plotted for three probes versus axial distance, Z, for a range of about 24 mm. For all curves shown in Fig. 10, each respond curve starts from a near zero value and reaches a maximum at a particular axial distance and then drops slowly to a minimum of near zero value. From this comparison three points can be concluded.

First, the dead region distance is smaller for the RS, which is about 2 mm, next for EF is about 3 mm and for the TS is the highest about 4 mm. Second point and perhaps the most important one, is the difference of the position of the peak intensity curves. For RS the peak position is at about 3 mm, for EF about 4.5 mm and finally for TS is at about 5.5 mm. The third notable points of this comparison are the variation of the intensity maximum values and the bandwidths (FWHM) values for different respond curves. As can be seen in Fig. 10, the amount of the intensity peaks remain almost constant (0.58) while the curve bandwidth (FWHM) is smallest for RS (2.4 mm), next for EF (2.7 mm) and finally for TS is the highest value (3.1 mm) for the assumed input values.

## DISCUSSION

Simulation results reveal some points that are discussed in more detail in this section. As can be seen in results, the respond curve includes three parts, the first and second region for increasing intensity and the third region for decrease in reflected light intensity as a function of the axial distance. From simulation results four general cases can be recognized. First, when there is no crossing between the two light cones (dead region) and the reflected intensity is zero. When there is a crossing between the two coins two cases can happen (either AB, above the horizontal cross section line CD; or AB below the cross section line) and the crossing area can increase from zero to a maximum value of T-fiber core area. When the circle is totally inside the spot light circle, then the amount of cross section $\Delta S$ is always a constant but the intensity of the received light in this area is decreased by increasing the axial distance.

For example result shown in Fig. 3 displays the respond curves of the EF double-fiber design computed from the Eq. 2 and 6 for the first rising region of the intensity curve and for the second region from Eq. 11. Two points can be concluded from the theoretical results shown here for different t values. First point is that the peak of the respond curve is shifted towards a larger distance as t increases. Second point is that for the first increasing part of the intensity curve, the probe with the smaller fiber-to-fiber t distance shows a sharper increase in comparison with that of the large fiber-to-fiber distance. As can seen in Fig. 3, the decay for the second region of the respond curve is about the same for all cases and the overall curve bandwidth for larger t is a little wider than for the smaller t values.

Fibers core and overall size and as a result the fiber-to-fiber distance has a great impact on the probe sensitivity and dynamic range. Fiber core radius and fiber overall size play also an important role in the maximum intensity and the bandwidth of the respond curve of such a probe. The length difference in the transmitting and receiving fibers is crucial and shifts the place of the intensity maximums in the respond curves. For TS and RS probe designs in respect to the EF case, the length difference shifts the maximum with respect to the EF for the TS design towards higher distance while for the RS design moves the place of maximum towards a shorter axial distance.

For all designs, dead region is controlled by parameters t, NA, but r has little effect in this respect. Maximum place of the intensity curve is governed mainly by t and NA. Maximum peak value of the intensity curve is governed mainly by r and NA. The bandwidth (FWHM) of the respond curve is controlled by t, NA and r values. It must be pointed out that since the core and cladding are the same for all three arrangements, thus the noted difference in Fig. 10 is only due to the length difference. The parameter w denoted for the length difference mainly controls the dead region, the place of intensity maximum and the bandwidth (FWHM) of the intensity curve.

Finally, the simulated respond curves are very similar to the experimental respond curve observed in the previous experimental studies. In general the developed theoretical formulas and algorithms effectively describe the performance of double-fiber probes suitable for

reflection/displacement sensors. A similar behavior is noted in experimental measured intensity as shown in Fig. 3 of Reference by Golnabi and Azimi (2008) for the sensor deign using the EF fiber probe. Given simulation results are in support of the previous ones and there is no contradiction in results. From practical point of view all the three arrangements simulated here are very easy to fabricate and offer a good size probe for sensing purposes depending on the application requirements. The EF arrangement provides good results for the sensing operation such as reflection or displacement measurements. However, the RS probe geometry offers a better design with the less dead region in comparison with the EF and TS designs as shown in Fig. 10. It must be pointed out that other geometries can be used for displacement sensing. More details about such designs in term of performance evaluation can be found in literature (Golnabi, 1999, 2000b).

## CONCLUSIONS

This article has described the simulation results for operation of three different double fiber probes. It was shown that presented information can be useful in design and operation of such non-contact sensor systems that can be used in a variety of applications. The reported simulation results reveal the following conclusions:

- **Effect of t:** This parameter controls the dead region distance and it is increased by increasing the t value. Controls the position of the maximum in intensity curve. Any increase of t increases the place of the peak. By increasing the t value the amount of the intensity peak remains nearly constant while the curve bandwidth (FWHM) is increased
- **Effect of r:** Controls the position of the peak in intensity respond curve. By increasing the r value the peak is shifted towards higher axial distance values. Also important point is the increase of the peak intensity as a result of the increase in r. By increasing the r value the intensity curve bandwidth (FWHM) is increased accordingly. The parameter r has little effect on the dead region range and by changing the fiber core radius the dead region distance remains almost constant
- **Effect of NA:** By increasing the NA value three major changes occur in the intensity plots. First, the dead region distance is decreased by increasing the NA value. Second point and the most important effect, is the shift of the peak intensity to shorter distances by an increase in the NA value. By increasing the NA value the amount of the intensity peak is slightly reduced while the curve bandwidth (FWHM) is considerably reduced by increasing the NA value
- **Effect of w:** First, For TS and RS designs the dead region distance is increased by increasing the w value. Second, the dead region distance is smaller for the RS, next for EF (w = 0) and for the TS is the highest. Third point and perhaps the most important ones, is the difference of the position of the peaks in intensity curves. For RS the peak position occurs at shorter axial distance, next for EF and finally for TS occurs at larger distances. The fourth notable points of this comparison are the variation of the intensity maximum values and the bandwidths (FWHM) values for different respond curves. The amount of the intensity peaks remain almost constant for three designs while the curve bandwidth (FWHM) is smallest for RS, next for EF and finally the TS design has the largest value

## ACKNOWLEDGMENT

This study was supported in part by the Sharif University of Technology Research program. The authors gratefully acknowledge the grant money devoted to this research (Grant No. 3104).

## REFERENCES

Babchenko, A. and J. Maryles, 2007. Graded-index plastic optical fiber for deformation sensing. Opt. Lasers Eng., 45: 757-760.

Baptista, J.M., SF. Santos, G. Rego, O. Frazão and J.L. Santos, 2006. Micro-displacement or bending measurement using a long-period fibre grating in a self-referenced fibre optic intensity sensor. Opt. Commun., 260: 8-11.

Donlagić, D. and E. Cibula, 2005. An all-fiber scanning interferometer with a large optical path length difference. Opt. Lasers Eng., 43: 619-623.

Golnabi, H., 1999. Design and operation of different optical-fiber sensors for displacement measurements. Rev. Sci. Instrum., 70: 2875-2879.

Golnabi, H., 2000a. Fiber optic displacement sensor using a coated lens optic. Rev. Sci. Instrum., 71: 4314-4318.

Golnabi, H., 2000b. Simulation of the interferometric sensors for pressure and temperature measurements. Rev. Sci. Instrum., 71: 1608-1613.

Golnabi, H., 2002. Mass measurement using intensity modulated optical fiber sensor. Opt. Lasers Eng., 38: 537-548.

Golnabi, H. and R. Jafari, 2006. Design and performance of an optical fiber sensor based on light leakage. Rev. Sci. Instrum., 77: 066103-066103-3.

Golnabi, H. and P. Azimi, 2007. Design and performance of a plastic optical fiber leakage sensor. Opt. Laser Technol., 39: 1346-1350.

Golnabi, H., M. Bahar, M. Razani, M. Abrishami and A. Asadpour, 2007. Design and operation of an evanescent optical fiber sensor. Opt. Lasers Eng., 45: 12-18.

Golnabi, H. and P. Azimi, 2008. Design and operation of a double-fiber displacement sensor. Optics Commun., 281: 614-620.

Peng, P.C., K.M. Feng, W.R. Peng, H.Y. Chiou, C.C. Chang and S. Chi, 2005. Long-distance fiber grating sensor system using a fiber ring laser with EDWA and SOA. Opt. Commun., 252: 127-131.

Qiu, T., L.S. Kuo and H.C. Yeh, 2004. A novel type of fiber optic displacement sensor based on Gaussian beam interference. Opt. Commun., 234: 163-168.

Weinert, A., 1999. Plastic Optical Fibers Principles, Compounds, Installation. Wiley-VCH., Weinheim, pp: 154.

Yuan, B., H.M. Yan and X.Q. Cao, 2009. A new subdivision method for grating based displacement sensor using image array. Opt. Lasers Eng., 47: 90-95.